

Ionic size effects to molecular solvation energy and to ion current across a channel resulted from the nonuniform size-modified PNP equations

Yu Qiao, Bin Tu, and Benzhuo Lu^{a)}

State Key Laboratory of Scientific and Engineering Computing, Institute of Computational Mathematics and Scientific Engineering Computing, National Center for Mathematics and Interdisciplinary Sciences, Academy of Mathematics and Systems Science, Chinese Academy of Sciences, Beijing 100190, China

(Received 9 February 2014; accepted 10 April 2014; published online 2 May 2014)

Ionic finite size can impose considerable effects to both the equilibrium and non-equilibrium properties of a solvated molecular system, such as the solvation energy, ionic concentration, and transport in a channel. As discussed in our former work [B. Lu and Y. C. Zhou, *Biophys. J.* **100**, 2475 (2011)], a class of size-modified Poisson-Boltzmann (PB)/Poisson-Nernst-Planck (PNP) models can be uniformly studied through the general nonuniform size-modified PNP (SMPNP) equations deduced from the extended free energy functional of Borukhov *et al.* [I. Borukhov, D. Andelman, and H. Orland, *Phys. Rev. Lett.* **79**, 435 (1997)] This work focuses on the nonuniform size effects to molecular solvation energy and to ion current across a channel for real biomolecular systems. The main contributions are: (1) we prove that for solvation energy calculation with nonuniform size effects (through equilibrium SMPNP simulation), there exists a simplified approximation formulation which is the same as the widely used one in PB community. This approximate form avoids integration over the whole domain and makes energy calculations convenient. (2) Numerical calculations show that ionic size effects tend to negate the solvation effects, which indicates that a higher molecular solvation energy (lower absolute value) is to be predicted when ionic size effects are considered. For both calculations on a protein and a DNA fragment systems in a 0.5M 1:1 ionic solution, a difference about 10 kcal/mol in solvation energies is found between the PB and the SMPNP predictions. Moreover, it is observed that the solvation energy decreases as ionic strength increases, which behavior is similar as those predicted by the traditional PB equation (without size effect) and by the uniform size-modified Poisson-Boltzmann equation. (3) Nonequilibrium SMPNP simulations of ion permeation through a gramicidin A channel show that the ionic size effects lead to reduced ion current inside the channel compared with the results without considering size effects. As a component of the current, the drift term is the main contribution to the total current. The ionic size effects to the total current almost come through the drift term, and have little influence on the diffusion terms in SMPNP. © 2014 AIP Publishing LLC. [<http://dx.doi.org/10.1063/1.4872330>]

I. INTRODUCTION

Among the theoretical approaches to understand molecular solvation properties, the implicit continuum model represented by the Poisson-Boltzmann (PB) equation is a rather widely used method, due to its simplicity of computation and successful application to many systems.^{3–6} In spite of its wide application in describing the equilibrium state of aqueous salt solution around a molecule, the usual PB equation neglects ionic finite size effects (volume exclusion) and other ion-ion correlations^{7–12} which can lead to unreasonably high, i.e., oversaturated concentrations of counter ions in the vicinity of molecular surface.^{1,2}

Size effects can be incorporated to the continuum model to cope with this problem to some extent, and within a mean-field framework, the numerical tractability for 3D computations can be maintained as well. Borukhov *et al.*^{2,13} presented a uniform size-modified Poisson-Boltzmann (SMPB)

equation through variation of an electrostatic free energy. In contrast with traditional energy form derived by Sharp *et al.*,¹⁴ an additional solvent entropy term, representing the unfavorable energy modeling the over-packing or crowding of ions and solvent molecules, is introduced to form a new energy functional. The new functional leads to a result that in equilibrium condition, ion concentrations can be expressed explicitly by potentials, bulk concentration, and ionic sizes, which thereby leads to the uniform SMPB. Numerical results show a great decrease of counter ions for a planar surface model when uniform ion size is applied. Using the same SMPB, Silalahi *et al.*¹⁵ have compared predictions of the equation and that of the nonlinear Poisson-Boltzmann equation (NPB) for a low-dielectric charged spherical cavity in an aqueous salt solution. Chu *et al.*¹⁶ extended the above uniform size model to include two different sizes of ion species and gave an explicit SMPB form and used it to study ion binding to DNA duplexes. Their results show good agreement with experimental data for monovalent ion when concentration is lower than 150 mM. However, when three or more sizes appear in the model, explicit form of ionic concentration as function of

^{a)} Author to whom correspondence should be addressed. Electronic mail: bzlu@lsec.cc.ac.cn

potential and ionic size does not exist. To avoid the difficulty, one of our authors¹ considered the more general electro-diffusion process by deriving a set of size-modified Poisson-Nernst-Planck (SMPNP) equations from a generalized energy functional of Borukhov *et al.* with nonuniform sizes. The SMPNP naturally treats arbitrary number of nonuniform sizes, and can be applied to describe both equilibrium state and non-equilibrium process of ionic solution.¹ The equilibrium solution of SMPNP has been proved and demonstrated to be exactly reduced to the SMPB situation.¹ The paper also provided a concrete instruction on how to obtain SMPB results from solution of SMPNP and studied the size effects to ion concentrations and diffusion reaction rate for a spherical cavity case. Boschitsch *et al.*¹⁷ derived an approach to study the nonuniform SMPB through simple statistical mechanics principles, and investigated ionic concentrations, potentials, and electrostatic free energy for a spherical cavity and a DNA structure cases. The dependence of energy over logarithm of bulk ionic concentration (SK) was originally derived by Sharp *et al.* for PB equation.^{18,19} This salt dependence has also been extended to SMPB model with uniform ion size case in the works by Fenley *et al.*^{15,20} They recently also conducted a parameterization study on molecular surface definition for the uniform SMPB model.²¹ Li *et al.*^{22–26} presented some mathematical analysis on the energy functional for both uniform and nonuniform SMPB and implemented numerical calculations on a sphere model.

We noticed that for this class of ion size-modified model, almost all of the above mentioned recent works were performed on spherical cavity cases, and most of the conclusions are derived under conditions of uniform ionic size. This paper, by using the SMPNP, will treat the general nonuniform size case, and investigate the size effects to solvation energy for protein and DNA systems. By mathematical analysis of the energy functional with general nonuniform sizes, we find that an approximate energy formulation exists, which is exactly the same form as practically used in almost all the PB softwares in the community. The approximation form greatly simplifies the energy calculations. However, we will show that the traditional PB calculation is a third-order approximation, whereas the same form for SMPNP/SMPB energy calculation is a (at least) second order approximation. Solvation energy calculations will be performed and studied on a sphere cavity, a DNA fragment, and an acetylcholinesterase (AChE) system by solving the equilibrium SMPNP using the technique mentioned in our previous work.¹

As aforementioned, since SMPNP also has advantage to be able to describe the non-equilibrium electro-diffusion process, we will also use it to study the ion current in an ion channel. In particular, the size effects embedded in this model will be investigated in detail. Ion channel is a kind of protein on the membrane controlling many crucial processes in cells by allowing ions, such as sodium, potassium, and calcium, passing through the membrane from one side to the other side. Many experimental and computational techniques are developed to investigate the structures and ionic conductances of ion channels.^{27–37} Among these, the PNP equations which couple the electrostatics with the diffusion process, is one of the popular theoretical methods used to simulate 3D

ion channel systems.^{37–40} However, neglecting the discrete particle effects is a drawback of PNP model in modeling real channel systems. Size effects have long been studied and incorporated into the electro-diffusion process.^{1,11,41–44} Here, we will employ the SMPNP to simulate ion transport through an ion channel, and dissect the size effects into different contributions as compared with the PNP predictions.

The paper is organized as follows. In Sec. II, a brief description about the nonuniform size model is given at first and then we deduce the solvation energy, its approximate formula, and salt dependence. At last, numerical calculation is briefly introduced. In Sec. III, we will compare the accurate and approximate solvation energies calculated from PB and nonuniform SMPNP for a spherical cavity, a DNA fragment, and an AChE system. In the second part of the results section, the ion current, as well as its different components are plotted against membrane potentials with and without size effects for a gramicidin A (gA) channel. Conclusions are summarized in Sec. IV.

II. METHOD

A. Model description

For molecular solvation study, the computational region Ω is divided into two parts, the molecular region Ω_m and the solvent region Ω_s , surrounding the molecule. The molecule is constituted of N atoms and the solvent contains K ion species. The Nernst-Planck equations are defined only in the solvent region, while the Poisson equation in the whole region. The concrete form of SMPNP is¹

$$\frac{\partial c_i(r)}{\partial t} = -\nabla \cdot J_i(r), \quad \text{in } \Omega_s, \quad i = 1, \dots, K, \quad (1)$$

$$\nabla \cdot \epsilon(r)\nabla\phi(r) + \rho^f + \rho^{ion}(r) = 0, \quad \text{in } \Omega, \quad (2)$$

where

$$J_i(r) = -D_i(r)(\nabla c_i(r) + \frac{k_i c_i(r)}{1 - \sum_l a_l^3 c_l(r)} \sum_l a_l^3 \nabla c_l(r) + \beta c_i(r) q_i \nabla \phi(r)), \quad (3)$$

$$\rho^f = \sum_{i=1}^N Q_i \delta(r - r_i), \quad (4)$$

$$\rho^{ion}(r) = \sum_{i=1}^K c_i(r) q_i, \quad (5)$$

$$k_i = \frac{a_i^3}{a_0^3}, \quad (6)$$

c_i and ϕ represent ionic concentration and potential to be solved, D_i is the diffusion coefficient of the i th ion species, a_i and a_0 denote the sizes of the i th ion species and water molecule, respectively, β is defined as $\frac{1}{k_B T}$, where k_B is the Boltzmann constant and T is the absolute temperature, q_i is the ionic charge of the i th ion species in the solvent, Q_i is the

i th atom's charge in the molecule, and $\epsilon = \epsilon_r \epsilon_0$ represents the dielectric permittivity in which ϵ_r is the relative permittivity and ϵ_0 is the vacuum permittivity. In this work, the relative permittivities are 2 in the molecular region and 78 in the solvent region. The temperature is 298 K. Here we only study the steady state $\frac{\partial c_i(r)}{\partial t} = 0$. When the second term of $J_i(r)$ is removed, SMPNP become PNP equations. It is not difficult to find that for equilibrium state ($J_i = 0$ everywhere), PNP can be reduced to NPB in symmetric 1:1 salt solution,

$$-\nabla \cdot (\epsilon(r) \nabla \phi(r)) + \bar{\kappa}^2 \left(\frac{k_B T \epsilon_0}{e_c} \right) \sinh \left(\frac{e_c \phi(r)}{k_B T} \right) = \sum_{i=1}^N Q_i \delta(r - r_i), \quad \text{in } \Omega, \quad (7)$$

where e_c is the elementary charge, $\bar{\kappa}^2 = \epsilon_s \kappa^2$, $\kappa^2 = 8.48 \frac{I_s}{\epsilon_s} \text{ \AA}^{-2}$, I_s is the ionic strength defined by $\frac{1}{2} \sum_{i=1}^K c_i z_i^2$ (z_i is the valence of the i th ion species) and is measured in unit of mol/l, and ϵ_s is the relative dielectric constant of the solvent.

It is clear that arbitrarily nonuniform ionic sizes can be naturally treated in above SMPNP model. When general nonuniform size effects are incorporated in the continuum model, the explicit form of ionic concentration as a function of potential cannot be found. Thus we cannot derive an explicit SMPB by simply substituting the ionic concentration expressions in a Poisson equation. Using the relation of SMPB and SMPNP discussed in paper,¹ we can get SMPB results from the solution of SMPNP by making sure no ion flux across the interface between molecule and solvent. We denote the interface by Γ_m and the boundary condition for SMPB is

$$J_i \cdot n = 0, \quad \text{on } \Gamma_m, \quad i = 1, \dots, K, \quad (8)$$

where n is the outward unit normal vector of the molecular surface. For SMPB calculation, the other boundary conditions are set the same as in PB calculation.

In ion channel simulating, there is an additional part, represented by the membrane, in the computational region. The PNP and SMPNP simulations, including the treatment of these regions, the boundary conditions and related coefficient settings, can be referred to the paper of Tu *et al.*³⁸

B. Electrostatic energies and their approximate computations

Electrostatic solvation energy ΔG_{ele} is one of the properties that we care most about for biomolecular electrostatics.³⁻⁵ For a molecule solvated in ionic solution, the electrostatic solvation energy can be defined as

$$\Delta G_{ele} = G_{sys} - G_{ref}, \quad (9)$$

where G_{sys} is the electrostatic free energy of the biomolecular system in the solvated state, and G_{ref} is the sum of biomolecular electrostatic energy in vacuum (with a homogenous relative dielectric constant ϵ_m) and the energy of the ionic solution with existing cavity formed by the biomolecule (the second part is taken as a reference state and incorporated into the G_{sys} component in following analysis). The solvation procedure is

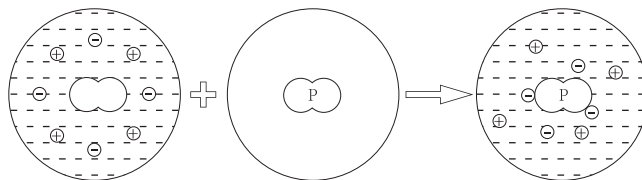


FIG. 1. Solvation energy of a biomolecular system. The final state is the biomolecule in ionic solution and the primitive state is constituted of biomolecule in vacuum and the ionic solution with existing of a cavity formed by the biomolecule.

illustrated in Figure 1. In the following part of this subsection, we will study the accurate and approximate expressions of electrostatic free energy and solvation energy in PB model in the first place. For the SMPNP, we will first discuss the accurate expressions of electrostatic free energy and solvation energy, and then deduce the approximate calculations by replacing the concentrations with their Taylor expansions.

In PB model, Sharp and Honig gave the following expression of electrostatic free energy through the calculus of variation:¹⁴

$$G_{sys} = \int_{\Omega} \left\{ \rho^f \phi - \frac{1}{2} \epsilon |\nabla \phi|^2 - \beta^{-1} c_b [2 \cosh(-e_c \beta \phi) - 2] \right\} dV, \quad (10)$$

where c_b is the bulk concentration. It is constituted of three parts, with the first one representing the contribution of point charges in the molecule, the second representing the contribution of electrostatics, and the last representing the osmotic pressure ($\Delta \Pi$). This energy is widely studied in many researches.^{6, 18, 19} For general ionic distributions, the electrostatic free energy of the biomolecular system is

$$G_{sys} = \int \left\{ \frac{1}{2} \rho \phi + \beta^{-1} \sum_{i=1}^K c_i [\ln(\Lambda^3 c_i) - 1] - \sum_{i=1}^K c_i \mu_i \right\} dV \quad (11)$$

or

$$G_{sys} = \int \left\{ \frac{1}{2} \epsilon |\nabla \phi|^2 + \beta^{-1} \sum_{i=1}^K c_i [\ln(\Lambda^3 c_i) - 1] - \sum_{i=1}^K c_i \mu_i \right\} dV, \quad (12)$$

where $\rho = \rho^f + \rho^{ion}$, Λ is the thermal de Broglie wavelength, and μ_i is the chemical potential for the i th ion species. Equation (12) can be derived from Eq. (11) through integration by parts. The following will show that Eq. (11) can be reduced to Eq. (10) for 1:1 symmetric ionic solution in equilibrium state.

Using equilibrium condition $\frac{\delta G_{sys}}{\delta c_i} = 0$ for the energy form defined in Eq. (11), we can obtain the following expression of c_i :

$$c_i = \Lambda^{-3} e^{\beta \mu_i} e^{-\beta q_i \phi} = c_{bi} e^{-\beta q_i \phi}, \quad (13)$$

where c_{bi} is the bulk concentration of the i th ion species. The second equivalent holds considering the condition that c_i approaches its bulk concentration at infinity where the potential vanishes. Substituting c_i with this expression in Eq. (11), we get

$$\begin{aligned} G_{sys} &= \int \left\{ \rho^f \phi + \rho^{ion} \phi - \frac{1}{2} \epsilon |\nabla \phi|^2 \right. \\ &\quad \left. + \beta^{-1} \sum_{i=1}^K c_i (\beta \mu_i - \beta q_i \phi - 1) - \sum_{i=1}^k c_i \mu_i \right\} dV \\ &= \int \left\{ \rho^f \phi - \frac{1}{2} \epsilon |\nabla \phi|^2 - \beta^{-1} \sum_{i=1}^K c_{bi} e^{-\beta q_i \phi} \right\} dV. \end{aligned} \quad (14)$$

Take $\phi = 0$ as a reference state and hence,

$$G_{sys} = \int \left\{ \rho^f \phi - \frac{1}{2} \epsilon |\nabla \phi|^2 - \beta^{-1} \sum_{i=1}^K c_{bi} (e^{-\beta q_i \phi} - 1) \right\} dV. \quad (15)$$

This equation is the same one as given by Sharp *et al.* for the NPB equation.

Electrostatic solvation energy can then be calculated as

$$\begin{aligned} \Delta G_{ele} &= - \int \left\{ \frac{1}{2} \rho^{ion} \phi^{sys} + \beta^{-1} \sum_{i=1}^K c_{bi} (e^{-\beta q_i \phi^{sys}} - 1) \right\} dV \\ &\quad + \frac{1}{2} \sum_{i=1}^N Q_i (\phi^{sys}(r_i) - \phi^{ref}(r_i)), \end{aligned} \quad (16)$$

where ϕ^{sys} and ϕ^{ref} are the potential in the solvated and vacuum state, respectively. Nevertheless, a simplified and approximate formula of ΔG_{ele} , denoted as

$$\Delta G_{ele}^{appr} = \frac{1}{2} \sum_{i=1}^N Q_i (\phi^{sys}(r_i) - \phi^{ref}(r_i)), \quad (17)$$

is widely used in PB solvers and program packages, such as DelPhi,⁴⁵ PBEQ,⁴⁶ and APBS⁴⁷ in biophysical and computational chemistry communities. This is because when ion concentrations obey Boltzmann distribution, the electrostatic free energy can be approximated by

$$G_{sys}^{appr} = \frac{1}{2} \int \rho^f \phi dV = \frac{1}{2} \sum_{i=1}^N Q_i \phi(r_i). \quad (18)$$

The reasonableness of Eq. (18) can be seen in following derivation:

$$\begin{aligned} G_{sys} &= \int \left\{ \rho^f \phi - \frac{1}{2} \epsilon |\nabla \phi|^2 - \beta^{-1} \sum_{i=1}^K c_{bi} (e^{-\beta q_i \phi} - 1) \right\} dV \\ &= \int \left\{ \rho^f \phi - \frac{1}{2} (\rho^f + \rho^{ion}) \phi \right. \\ &\quad \left. - \beta^{-1} \sum_{i=1}^K c_{bi} (e^{-\beta q_i \phi} - 1) \right\} dV \\ &= \int \left\{ \frac{1}{2} \rho^f \phi - \frac{1}{2} \sum_{i=1}^K q_i c_i \phi \right. \\ &\quad \left. - \beta^{-1} \sum_{i=1}^K c_{bi} (e^{-\beta q_i \phi} - 1) \right\} dV \\ &= \int \left\{ \frac{1}{2} \rho^f \phi - \frac{1}{2} \sum_{i=1}^K q_i c_{bi} [1 - \beta q_i \phi + O(\phi^2)] \phi \right. \\ &\quad \left. - \beta^{-1} \sum_{i=1}^K c_{bi} \left[1 - \beta q_i \phi + \frac{1}{2} (\beta q_i \phi)^2 \right. \right. \\ &\quad \left. \left. + O(\phi^3) - 1 \right] \right\} dV \\ &= \int \left\{ \frac{1}{2} \rho^f \phi + \frac{1}{2} \sum_{i=1}^K q_i c_{bi} \phi + O(\phi^3) \right\} dV \\ &= G_{sys}^{appr} + \int O(\phi^3) dV. \end{aligned} \quad (19)$$

The neutrality condition $\sum_{i=1}^K q_i c_{bi} = 0$ is applied to the second term in the integral. Eq. (19) indicates that the traditional energy calculation formula in usual PB solvers is an approximation neglecting the third order terms in the energy integral. Based on this approximate electrostatic free energy expression, we can obtain the approximate solvation energy formulation in Eq. (17). In accurate energy calculation, integration over the whole domain has to be performed, while the approximate one is only performed on finite points, which makes it much easier and more convenient to realize the solvation energy computing.

For an ionic size-modified model by extending the work of Borukhov *et al.*,² an additional entropy term is added to make a modification to the electrostatic free energy,^{1,2,13,15,25}

$$\begin{aligned} G_{sys} &= \int \left\{ \frac{1}{2} \rho \phi + \beta^{-1} \sum_{i=1}^K c_i [\ln(c_i a_i^3) - 1] - \sum_{i=1}^K c_i \mu_i \right. \\ &\quad \left. + \frac{\beta^{-1}}{a_0^3} \left(1 - \sum_{i=1}^K c_i a_i^3 \right) \left[\ln \left(1 - \sum_{i=1}^K c_i a_i^3 \right) - 1 \right] \right\} dV, \end{aligned} \quad (20)$$

where a_0 stands for the size of water molecule and a_i for the i th ion species. In equilibrium condition, the following

equation holds:

$$\frac{\delta G_{sys}}{\delta c_i} = 0. \quad (21)$$

Hence,

$$q_i \phi + \beta^{-1} \left[\ln(c_i a_i^3) - \frac{a_i^3}{a_0^3} \ln \left(1 - \sum_{i=1}^K c_i a_i^3 \right) \right] - \mu_i = 0. \quad (22)$$

From above equations, we have the expression of μ_i and plug it into electrostatic free energy and obtain

$$\begin{aligned} G_{sys} = & \int \left\{ -\frac{1}{2} \epsilon |\nabla \phi|^2 + \rho^f \phi + \sum_{i=1}^K c_i q_i \phi \right. \\ & + \beta^{-1} \sum_{i=1}^K c_i \ln(c_i a_i^3) - \beta^{-1} \sum_{i=1}^K c_i - \sum_{i=1}^K c_i q_i \phi \\ & + \frac{\beta^{-1}}{a_0^3} \ln \left(1 - \sum_{i=1}^K c_i a_i^3 \right) - \beta^{-1} \sum_{i=1}^K c_i \\ & \times \left[\ln(c_i a_i^3) - \frac{a_i^3}{a_0^3} \ln \left(1 - \sum_{i=1}^K c_i a_i^3 \right) \right] \\ & - \beta^{-1} \sum_{i=1}^K c_i \frac{a_i^3}{a_0^3} \ln \left(1 - \sum_{i=1}^K c_i a_i^3 \right) - \frac{\beta^{-1}}{a_0^3} \\ & \left. + \beta^{-1} \sum_{i=1}^K c_i \frac{a_i^3}{a_0^3} \right\} dV \\ = & \int \left\{ -\frac{1}{2} \epsilon |\nabla \phi|^2 + \rho^f \phi + \frac{\beta^{-1}}{a_0^3} \ln \left(1 - \sum_{i=1}^K c_i a_i^3 \right) \right. \\ & \left. + \beta^{-1} \sum_{i=1}^K c_i \left(\frac{a_i^3}{a_0^3} - 1 \right) - \frac{\beta^{-1}}{a_0^3} \right\} dV. \quad (23) \end{aligned}$$

Taking $\phi = 0$ as a reference state, we have the final form of electrostatic free energy

$$\begin{aligned} G_{sys} = & \int \left\{ -\frac{1}{2} \epsilon |\nabla \phi|^2 + \rho^f \phi + \frac{\beta^{-1}}{a_0^3} \ln \frac{1-C}{1-C_0} \right. \\ & \left. + \beta^{-1} \sum_{i=1}^K (c_i - c_{bi}) \left(\frac{a_i^3}{a_0^3} - 1 \right) \right\} dV, \quad (24) \end{aligned}$$

where

$$C = \sum_{i=1}^K c_i a_i^3, \quad (25)$$

$$C_0 = \sum_{i=1}^K c_{bi} a_i^3. \quad (26)$$

When all sizes are taken to be the same value, the above form is the same as that in Ref. 15 for the uniform SMPB,

$$G_{sys} = \int \left\{ -\frac{1}{2} \epsilon |\nabla \phi|^2 + \rho^f \phi + \frac{\beta^{-1}}{a^3} \ln \frac{1-C}{1-C_0} \right\} dV. \quad (27)$$

Though quite different from that of PB, Eq. (27) can be reduced to Eq. (15) when $a \rightarrow 0$. In general nonuniform SMPB case, the electrostatic solvation energy is calculated by

$$\begin{aligned} \Delta G_{ele} = & \frac{1}{2} \int \left\{ -\rho^{ion} \phi^{sys} + \frac{\beta^{-1}}{a_0^3} \ln \frac{1-C}{1-C_0} \right. \\ & \left. + \beta^{-1} \sum_{i=1}^K (c_i - c_{bi}) \left(\frac{a_i^3}{a_0^3} - 1 \right) \right\} dV \\ & + \frac{1}{2} \sum_{i=1}^N Q_i (\phi^{sys}(r_i) - \phi^{ref}(r_i)). \quad (28) \end{aligned}$$

In the following, we will prove that a similar approximation form as in PB model exists for calculation of above general nonuniform size-modified solvation free energy.

The approximate electrostatic free energy calculation with size effects can be derived by substituting concentration c_i in Eq. (24) with its Taylor expansion with respect to potential ϕ at zero point. First define

$$c_0 a_0^3 = 1 - C. \quad (29)$$

According to our former study,¹ when ionic size effects are considered in the SMPNP, the modified ion chemical potential becomes $V_i = q_i \phi - \frac{k_i}{\beta} \ln(1 - \sum_{i=1}^K c_i a_i^3)$. In this sense, ionic concentration can be expressed by $\tilde{C}_i e^{-\beta V_i}$ where \tilde{C}_i is a constant needed to be determined. Using the boundary condition $c_i(\phi)|_{\Gamma_s} = c_i(0) = c_{bi}$ (Γ_s is the boundary of the computational region), we can obtain an implicit concentration relation with size effects

$$c_i = c_{bi} e^{-k_i \ln(1-C_0)} e^{-\beta q_i \phi + k_i \ln(1-C)}. \quad (30)$$

This general ion distribution formulation was also implied in the general Slotboom transformation for SMPNP.¹ Assuming the Taylor expansion of $\ln(1-C)$ with respect to ϕ at zero point is

$$\ln(1-C) = \ln(1-C_0) + A\phi + O(\phi^2), \quad (31)$$

where the unknown A is to be determined, we can then have the expansion c_i to order 2

$$c_i = c_{bi} (1 - \beta q_i \phi + k_i A \phi + O(\phi^2)). \quad (32)$$

Based upon this expansion, $\ln(1-C)$ can be written as

$$\begin{aligned} \ln(1-C) = & \ln(1-C_0) + \frac{1}{1-C_0} \\ & \times \left(\beta \phi \sum_{i=1}^K c_{bi} a_i^3 q_i - A \phi \sum_{i=1}^K c_{bi} a_i^3 k_i \right) + O(\phi^2). \quad (33) \end{aligned}$$

Comparing the coefficient of ϕ in Eqs. (31) and (33), we can get the expression of A and then the Taylor expansions of

$\ln(1-C)$ and c_i with respect to ϕ

$$\ln(1-C) = \ln(1-C_0) + \frac{\beta a_0^3 \sum_{i=1}^K c_{bi} a_i^3 q_i}{\sum_{i=0}^K c_{bi} a_i^6} \phi + O(\phi^2), \quad (34)$$

$$c_i = c_{bi} + \beta c_{bi} \left(\frac{a_i^3 \sum_{j=1}^K c_{bj} a_j^3 q_j}{\sum_{j=0}^K c_{bj} a_j^6} - q_i \right) \phi + O(\phi^2). \quad (35)$$

These expansions can also be concluded from the recent work of Li *et al.*²⁶ in exploring the modified Debye length due to ionic size effects. Denote $B_1 = -\frac{1}{2} \rho^{ion} \phi = -\frac{1}{2} \sum_{i=1}^K c_i q_i \phi$, then Eq. (35) leads to

$$\begin{aligned} B_1 &= -\frac{1}{2} \sum_{i=1}^K \left(c_{bi} q_i \phi - \beta c_{bi} q_i^2 \phi^2 \right. \\ &\quad \left. + \beta c_{bi} a_i^3 q_i \phi^2 \frac{\sum_{j=1}^K c_{bj} a_j^3 q_j}{\sum_{j=0}^K c_{bj} a_j^6} \right) + O(\phi^2) \\ &= -\frac{1}{2} \beta \left(\sum_{i=1}^K c_{bi} q_i^2 - \frac{(\sum_{i=1}^K c_{bi} a_i^3 q_i)^2}{\sum_{i=0}^K c_{bi} a_i^6} \right) \phi^2 + O(\phi^2) \\ &= O(\phi^2). \end{aligned} \quad (36)$$

Denote $B_2 = \frac{\beta^{-1}}{a_0^3} \ln \frac{1-C}{1-C_0}$, Eq. (34) then leads to

$$\begin{aligned} B_2 &= \frac{\beta^{-1}}{a_0^3} (\ln(1-C) - \ln(1-C_0)) \\ &= \frac{\beta^{-1}}{a_0^3} \left(\frac{\beta a_0^3 \sum_{i=1}^K c_{bi} a_i^3 q_i}{\sum_{i=0}^K c_{bi} a_i^6} \right) \phi + O(\phi^2) \\ &= \frac{\sum_{i=1}^K c_{bi} a_i^3 q_i}{\sum_{i=0}^K c_{bi} a_i^6} \phi + O(\phi^2). \end{aligned} \quad (37)$$

Denote $B_3 = \beta^{-1} \sum_{i=1}^K (c_i - c_{bi}) \left(\frac{a_i^3}{a_0^3} - 1 \right)$, then we have

$$\begin{aligned} B_3 &= \beta^{-1} \sum_{i=1}^K \beta c_{bi} \left(\left(\frac{a_i^3 \sum_{j=1}^K c_{bj} a_j^3 q_j}{\sum_{j=0}^K c_{bj} a_j^6} - q_i \right) \phi + O(\phi^2) \right) \\ &\quad \times \left(\frac{a_i^3}{a_0^3} - 1 \right) \\ &= \sum_{i=1}^K \left(-c_{bi} q_i \phi \frac{a_i^3}{a_0^3} + c_{bi} q_i \phi + c_{bi} a_i^6 \frac{\sum_{j=1}^K c_{bj} a_j^3 q_j}{a_0^3 \sum_{j=0}^K c_{bj} a_j^6} \right. \\ &\quad \left. - c_{bi} a_i^3 \frac{\sum_{j=1}^K c_{bj} a_j^3 q_j}{\sum_{j=0}^K c_{bj} a_j^6} \phi \right) + O(\phi^2) \\ &= -\frac{\sum_{i=1}^K c_{bi} a_i^3 q_i}{\sum_{i=0}^K c_{bi} a_i^6} \phi + O(\phi^2). \end{aligned} \quad (38)$$

Using Eqs. (36)–(38), and (24), we can deduce the following expression of G_{sys} with size effects:

$$\begin{aligned} G_{sys} &= \int \left\{ -\frac{1}{2} \epsilon |\nabla \phi|^2 + \rho^f \phi + B_2 + B_3 \right\} dV \\ &= \int \left\{ -\frac{1}{2} (\rho^f + \rho^{ion}) \phi + \rho^f \phi + \frac{\sum_{i=1}^K c_{bi} a_i^3 q_i}{\sum_{i=0}^K c_{bi} a_i^6} \phi \right. \\ &\quad \left. - \frac{\sum_{i=1}^K c_{bi} a_i^3 q_i}{\sum_{i=0}^K c_{bi} a_i^6} \phi + O(\phi^2) \right\} dV \\ &= \int \left\{ \frac{1}{2} \rho^f \phi + B_1 + O(\phi^2) \right\} dV \\ &= G_{sys}^{appr} + \int \{O(\phi^2)\} dV. \end{aligned} \quad (39)$$

It is straightforward that $G_{sys}^{appr} = \frac{1}{2} \sum_{i=1}^N Q_i \phi(r_i)$ can be a good approximate electrostatic free energy expression for both PB and SMPNP/SMPB models. Therefore, the approximate solvation energy defined by Eq. (17) can hold for the two models. However, it is worth noting that we can only prove here the simplified energy calculation form is (at least) a second order approximation for SMPNP, whereas for PB it is on the third order. The derivation indicates that when the potential is very high, the approximate energy calculation form may cause considerable error.

C. Salt dependence

In this subsection, the salt dependence, the derivative of electrostatic free energy with respect to the bulk ionic concentration is reviewed for the traditional PB and uniform SMPB equation. For symmetric 1:1 salt solution described by PB, Sharp *et al.* have shown¹⁸

$$\frac{dG_{sys}}{d\kappa} = -\frac{2}{\kappa} \Delta \Pi, \quad (40)$$

where $\Delta \Pi$ represents the osmotic pressure in electrostatic free energy. Silalahi *et al.*¹⁵ have given the derivative of electrostatic free energy with respect to $\log c_b$:

$$\frac{dG_{sys}}{d \log c_b} = -\Delta \Pi \quad (41)$$

for PB and

$$\frac{dG_{sys}}{d \log c_b} = -\frac{\beta^{-1}}{a^3} \int \frac{\xi}{1+\xi} dV \quad (42)$$

for uniform SMPB, where $\xi = a^3 \sum_{i=1}^K c_{bi} (e^{-\beta q_i \phi} - 1)$. From above equations, we notice that electrostatic free energies in PB and uniform SMPB decrease as bulk ionic concentration increases. However, in nonuniform size case, the electrostatic free energy and its salt dependence are much more complicated, and it seems difficult for us to arrive at a similar and an explicit conclusion. Here, we just consider a simple case, symmetric 1:1 salt solution, and give the following salt

dependence:

$$\begin{aligned} & \frac{dG_{sys}}{d \log c_b} \\ &= \int \left\{ c_b \left[-\rho^{ion} + \frac{1}{M} \left(\frac{a_1^3}{a_0^3} c_1 q_1 + c_2 q_2 \right) \right] \frac{d\phi}{dc_b} \right. \\ & \quad + c_b \left(1 - \frac{1}{M} \right) \frac{q_2}{a_2^3} \frac{d\phi}{dc_b} \\ & \quad - \frac{\beta^{-1}}{a_2^3} \left[\left(1 - \frac{1-C}{1-C_0} \frac{1}{M} \left(1 - \left(1 - \frac{a_2^3}{a_0^3} \right) \sum_{i=1}^k c_{bi} a_i^3 \right) \right) \right. \\ & \quad \left. - \frac{1}{M} \frac{a_2^3}{a_0^3} c_b a_1^3 R \left(\frac{c_2}{c_{b2}} \right)^v (1-v) \right] \\ & \quad \left. + \frac{1}{M} c_b c_2 q_2 P^{v-1} Q R (1-v) \right\} dV, \end{aligned} \quad (43)$$

where $v = \frac{a_1^3}{a_2^3}$, $P = c_2 a_2^3$, $Q = \frac{c_{b1} a_1^3}{(c_{b2} a_2^3)^v}$, $R = e^{-\beta(q_1 - v q_2)\phi}$, and $M = 1 - \left(1 - \frac{a_1^3}{a_0^3} \right) c_1 a_1^3 - \left(1 - \frac{a_2^3}{a_0^3} \right) c_2 a_2^3$. It is clear that this equation can be reduced to Eq. (42) when uniform size is applied. Unlike expressions for PB and uniform SMPB, this formula is constituted of more terms and it is hard to determine whether it is positive or negative. Nevertheless, in numerical computations as shown in Sec. III, a decrease of solvation energy from nonuniform SMPB results is observed as the bulk concentration increases.

D. Numerical calculation

To solve the partial differential equations, a finite element method is used to get numerical results of concentration and potential distributions that are involved in the solvation energy and current calculations. The algorithms are implemented with the parallel adaptive finite element package PHG.⁴⁸ The molecular surface mesh generating software TMSmesh^{49,50} which can handle large systems successfully is used to generate a manifold surface mesh. The program Tetgen⁵¹ is applied to generate the tetrahedral volume mesh. During numerical calculation, there are two main problems needed to be solved. The first one is the singular part representing biomolecule charge density in the Poisson equation of the SMPNP equations. A decomposition method⁵²⁻⁵⁴ is employed by resolving ϕ into three parts,

$$\phi = G + H + \phi_r. \quad (44)$$

G is the solution of equation $-\epsilon_m \Delta G = \rho^f$ confined to the molecular region Ω_m and H satisfies

$$\Delta H = 0, \quad \text{in } \Omega_m, \quad (45)$$

$$H = -G, \quad \text{on } \Gamma_m. \quad (46)$$

According to the Poisson equation, we can deduce the equation that ϕ_r satisfies. In addition, with this decomposition the

electrostatic solvation energies become

$$\begin{aligned} \Delta G_{ele} = & -\frac{1}{2} \int \left\{ \rho^{ion} \phi_r + \beta^{-1} \sum_{i=1}^K c_{bi} (e^{-\beta q_i \phi_r} - 1) \right\} dV \\ & + \frac{1}{2} \sum_{i=1}^N Q_i (H^i + \phi_r^i) \end{aligned} \quad (47)$$

for PB model,

$$\begin{aligned} \Delta G_{ele} = & \int \left\{ -\frac{1}{2} \rho^{ion} \phi_r + \frac{\beta^{-1}}{a_0^3} \ln \frac{1-C}{1-C_0} \right. \\ & \left. + \beta^{-1} \sum_{i=1}^K (c_i - c_{bi}) \left(\frac{a_i^3}{a_0^3} - 1 \right) \right\} dV \\ & + \frac{1}{2} \sum_{i=1}^N Q_i (H^i + \phi_r^i) \end{aligned} \quad (48)$$

for SMPNP/SMPB model, and

$$\Delta G_{ele}^{appr} = \frac{1}{2} \sum_{i=1}^N Q_i (H^i + \phi_r^i) \quad (49)$$

for both above models, where H^i and ϕ_r^i are the values of H and ϕ_r at the position of the i th atom in the biomolecule. Another difficulty in calculation is the nonlinearity resulting from size effects in the Nernst-Planck (NP) equations. We use Newton method to solve nonlinear problems, and use relaxation during the iteration between the coupled NP equations and the Poisson equation to guarantee the convergence of the algorithm.

III. RESULTS

In the following, the equilibrium SMPNP calculations are performed on a spherical cavity, a DNA fragment, and an acetylcholinesterase system to study the size effects to solvation energy in the first place. We then present nonequilibrium SMPNP simulation results on a gramicidin A channel system to investigate the size effects to ion current across the channel, with different components of the current studied explicitly. In ionic solution surrounding the biomolecule, only two ion species are considered in our calculation, one with charge $q_+ = e_c$ and the other with charge $q_- = -e_c$. To estimate the water molecule size a_0 involved in the size effects calculations, we can consider 1 l pure water completely filled with water molecule and every molecule is regarded as a cubic box of $a_0 \times a_0 \times a_0$. Then a_0 has the following value:

$$\begin{aligned} a_0 & \approx \left(\frac{10^{27} \text{ \AA}^3}{\frac{10^3 \text{ g}}{18 \text{ g/mol}} \times 6.02 \times 10^{23} \text{ mol}^{-1}} \right)^{\frac{1}{3}} \\ & = \left(\frac{180}{6.02} \right)^{\frac{1}{3}} \text{ \AA} \approx 3.1 \text{ \AA}. \end{aligned} \quad (50)$$

It is worth noting that the ionic sizes in SMPB/SMPNP models are not simply the values derived from a force field, instead, they should be obtained from an extensive fitting procedure, which is outside the scope of this work. For numerical

tests, if not specified, ionic sizes are chosen to be $a_+ = 2.3 \text{ \AA}$ and $a_- = 2.4 \text{ \AA}$. Considering the existence of hydration shell, a couple of hydrated ionic sizes, $a_+ = 4.8 \text{ \AA}$ and $a_- = 6.4 \text{ \AA}$, are also tested in the solvation calculations.

A. Size effects to solvation energy

In this subsection, we will show numerical results of the influence of size effects to solvation energy in a spherical model system, a DNA fragment, and an AChE protein system. A unit sphere carrying a charge e_c at the origin simulates the molecule in the sphere model with the solvent domain simulated in a spherical cavity of radius 200 \AA . There are 12 003 unknowns in the whole domain. The DNA fragment applied here contains a total charge of $-22e_c$ and is constituted of 778 atoms. The radius of solvent domain has the same as that of the sphere model, while the volume mesh has a total of 99 093 vertices. The AChE molecule is made up of 8362 atoms with its total charge amount being $-7.16e_c$. The total calculation region is a spherical region of radius 400 \AA , with 176 673 vertices in it.

When size effects are considered, ionic concentration under equilibrium state does not obey the Boltzmann distribution satisfied in PB any more. Denote ionic concentration in PB as

$$c_i^{PB} = c_{bi} e^{-\beta q_i \phi}. \quad (51)$$

In uniform SMPB, Borukhov *et al.* have given the following expression of ionic concentration:²

$$c_i^{SMPB} = \frac{c_i^{PB}}{1 + \xi}. \quad (52)$$

Nevertheless, for nonuniform SMPB we can only get the implicit relation of concentration defined in Eq. (30). Physically, ionic size effects avoid counter ions overcrowding in the vicinity of biomolecule. On the other hand, with less counter ions, less charges inside the molecule are neutralized and the electric field strength becomes stronger, which indicates more counter ions will be attracted and accumulated around the surface. These two opposite and balancing factors affect the final ionic concentration together. Figure 2(a) illustrates the counter-ion concentrations around the spherical cavity. The counter-ion concentration decreases significantly from 48.9 M to 11.4 M near the spherical surface when size effects are considered at 0.5 M . Potential around the surface is then influenced by the change of counter-ion concentration when size effects are involved, see Figure 2(b). The potentials in SMPB as shown in Figure 2(b) are higher than those in PB. These differences will lead to different solvation energies which can be calculated through expressions of ionic concentrations and potentials.

First, we will compare the accurate and approximate solvation energy calculations described in Sec. II. The solvation energies are calculated under a series of bulk concentrations, from 0.01 M to 0.09 M (with a step size of 0.01 M) and from 0.1 M to 1.0 M (with a step size of 0.1 M). For the spherical cavity the results are plotted in Figure 3. It is clearly seen that the approximate solvation energy calculation usually results in lower values than the accurate calculations in PB and

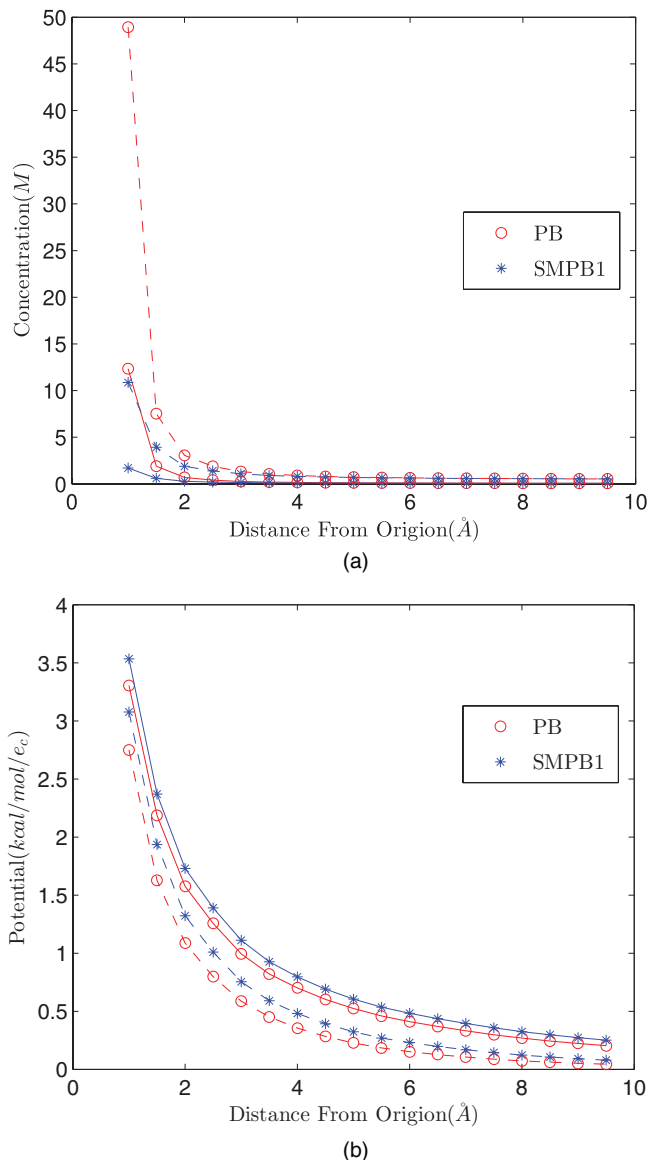


FIG. 2. (a) Counter-ion concentrations and (b) potential profiles around the unit spherical cavity at bulk concentrations 0.05 M (solid line) and 0.5 M (dashed line). In SMPB1, the ion sizes are $a_+ = 2.3 \text{ \AA}$ and $a_- = 2.4 \text{ \AA}$.

SMPB models in the cases of low ionic strength or small ionic sizes. Nevertheless, a noticeable phenomenon that the approximate energies are higher than the accurate ones is observed when larger (hydrated) ionic sizes are considered at bulk concentrations larger than 0.2 M , as shown in SMPB3 case in the figure. This also indicates that ionic sizes can impose significant influence on the biomolecular systems. In the spherical model, the difference between these two calculations for PB is no larger than 0.08 kcal/mol when bulk concentration is under 1 M . When size exclusion is considered, the difference is within a similar level, 0.09 kcal/mol . It is worth noting that though the integration region has a sufficiently large radius (200 \AA) of the outer boundary compared with the spherical cavity, the finite size of the computational domain Ω and the boundary conditions used in the simulations have little numerical influence to our energy computations and relevant conclusions. But for DNA system, it is found the difference

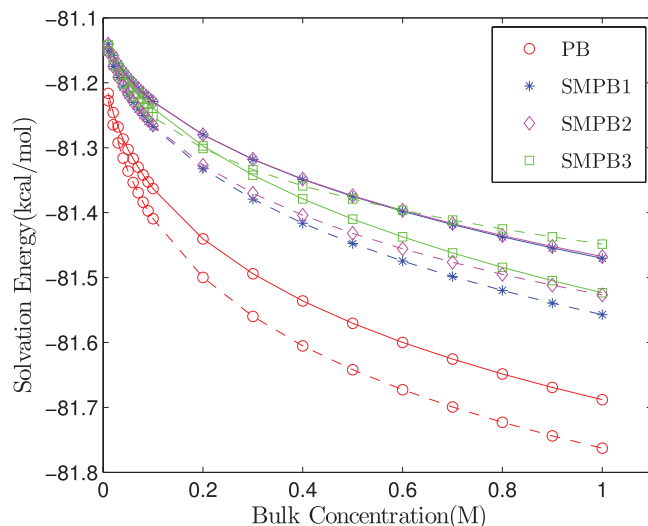


FIG. 3. Accurate and approximate solvation energies of the spherical cavity in SMPB and PB models. The solid lines stand for the accurate energy results (using Eqs. (47) and (48)), while the dashed for the approximate ones (using Eq. (49)). Three different pairs of ionic sizes are considered: (1) SMPB1: $a_+ = 2.3 \text{ \AA}$, $a_- = 2.4 \text{ \AA}$ (star); (2) SMPB2: $a_+ = 3.5 \text{ \AA}$, $a_- = 4.0 \text{ \AA}$ (diamond); and (3) SMPB3: $a_+ = 4.8 \text{ \AA}$, $a_- = 6.4 \text{ \AA}$ (square).

between the accurate and approximate energy calculations is within 5.42 kcal/mol and 9.59 kcal/mol for PB and SMPB, respectively (see Figure 4(a)). In addition, the difference becomes larger when ionic size effects are incorporated into the model. This may be due to the lower order of the energy approximation in SMPB model than that in PB model. For AChE system, the differences between accurate and approximate energy calculations are found to be within 2.61 kcal/mol and 3.99 kcal/mol in PB and SMPB, respectively (see Figure 4(b)). As implied by Eqs. (19) and (39), the approximation error in solvation energy computation for PB is smaller than that for SMPB. In addition, as shown in Figure 3 for spherical case and Figure 4 for DNA and AChE systems, larger ionic sizes (within a reasonable range) in SMPB more likely lead to higher solvation energies, hence result in more significant effects to solvation.

From these two figures, two additional phenomena are observed. One is that a similar trend of salt dependencies of the solvation energies (no matter approximate or accurate computations) is observed in all the sphere, DNA and AChE systems: the solvation energy decreases as the bulk ionic concentration increases. In the uniform size and zero size (without size effect) cases, Eqs. (41) and (42) already give a clearly theoretical prediction of such a phenomenon. However, similar conclusion seems cannot be reached straightforward from the salt dependence expression of Eq. (43) for the general nonuniform size case, though Eqs. (41) and (42) are special cases of Eq. (43). Therefore, we can only support by numerical experiments (and also from more other tests with different nonuniform size sets, not listed here) that it seems to be general to find a decreasing solvation energy along with the increasing ionic strength in the nonuniform SMPNP/SMPB model.

Another phenomenon is that the SMPB solvation energy is apparently higher than the PB one under a same con-

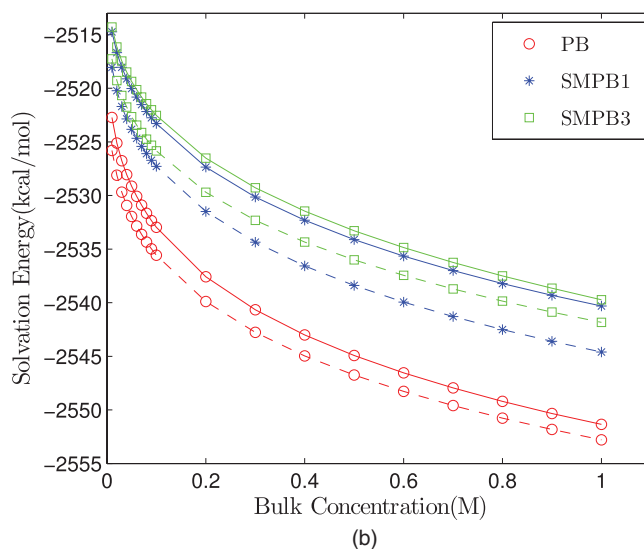
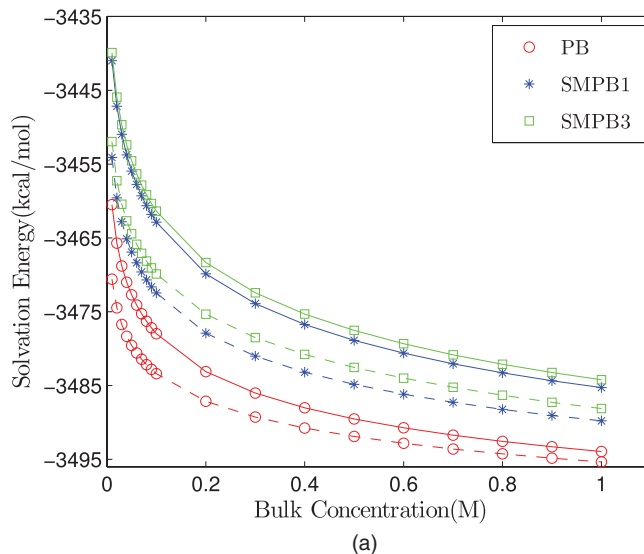


FIG. 4. Solvation energies in a symmetric 1:1 salt solution for (a) DNA and (b) AChE systems in various bulk concentrations. The solid and dashed lines have the similar meanings as in Figure 3. Two different pairs of ionic sizes are considered: (1) SMPB1: $a_+ = 2.3 \text{ \AA}$, $a_- = 2.4 \text{ \AA}$ (star); (2) SMPB3: $a_+ = 4.8 \text{ \AA}$, $a_- = 6.4 \text{ \AA}$ (square).

dition. At 0.5M, the difference is about 0.20 kcal/mol for sphere case, and about 10.64 kcal/mol and 10.31 kcal/mol for the DNA and AChE systems, respectively. When steric effects are incorporated, counter-ion concentration near molecular surface becomes smaller than that without size effect considered. As a result, this leads to a reduced screening (thereby stronger electric field) for the electrostatic interaction between biomolecule and ionic solution, which implies that the molecular solvation state with less concentrated counter-ion atmosphere becomes closer to the state in vacuum where screening vanishes. The solvation energy is usually negative. Therefore, in SMPB, the solvation energy (as definition, it is the energy difference between the solvated state and the vacuum state) becomes larger than in PB. This also means the absolute value of solvation energy with size effects considered becomes smaller than that without size effects considered, which are shown in Figures 3 and 4. The above

physical phenomenon can also be explained by the increase of Debye length (a measure of screening effect) in the SMPB model, which is proved in a recent work of Li *et al.*²⁶ They have derived the size-modified Debye length

$$\tilde{\lambda}_D^{-2} = \frac{\beta}{\epsilon} \left[\sum_i q_i^2 c_{bi} - \frac{(\sum_i q_i c_{bi} a_i^3)^2}{\sum_i c_{bi} a_i^6} \right]. \quad (53)$$

Compared to the classical Debye length λ_D that satisfies $\lambda_D^{-2} = \frac{\beta}{\epsilon} \sum_i c_{bi} q_i^2$, the size-modified Debye length $\tilde{\lambda}_D^{-2}$ is longer, but as calculated in Ref. 26, the modifications are not much significant in normal situations. This directly indicates an attenuation of screen effect, hence leads to stronger electric field as we declared above. However, we noticed an issue of this formulation, which may indicate a drawback of the theory or improperness of linearization of the SMPB/SMPNP model for uniform size case. When a special case of uniform size is considered, it is found that the size-modified Debye length $\tilde{\lambda}_D$ is equal to the classical Debye length λ_D , which means there is no any size effects included in the Debye length. This can be deduced from Eq. (53) by employing charge neutrality condition $\sum_i q_i c_{bi} = 0$. This means in Eq. (53), the uniform size effects do not make any change to the Debye length, which indicates that Eq. (53) cannot capture the influence of uniform ionic size effects, and the influence of ionic size effects is only observed when the ionic sizes are not identical. However, as shown by our previous physical explanations and numerical results, both uniform size and nonuniform sizes impose similar influences to ion concentrations, electrostatic screening, and solvation energy at a wide range of systems and settings.

B. Size effects to ion current across a channel

In this subsection, we concentrate on ionic size effects to the ion current-voltage characteristic of a channel system by adopting the same SMPNP model, but for nonequilibrium process simulation. Gramicidin A (gA) channel is simulated by solving the SMPNP equations. Unlike the above systems modeled in a spherical domain, gA is placed in a box of $30 \text{ \AA} \times 30 \text{ \AA} \times 45 \text{ \AA}$ with a total number of 22 793 vertices in the volume mesh discretization. The channel is aligned with the z direction.

In the method section, it is found that ion flux J_i with size effects has an additional diffusion component, compared to that without size effect. The current across a certain cut plane is subsequently calculated as

$$I_z = - \sum_{i=1}^K q_i \int D_i \times \left(\frac{\partial c_i}{\partial z} + \frac{k_i c_i}{1 - \sum_l a_l^3 c_l} \sum_l a_l^3 \frac{\partial c_l}{\partial z} + \frac{q_i}{k_B T} c_i \frac{\partial \phi}{\partial z} \right) dx dy \quad (54)$$

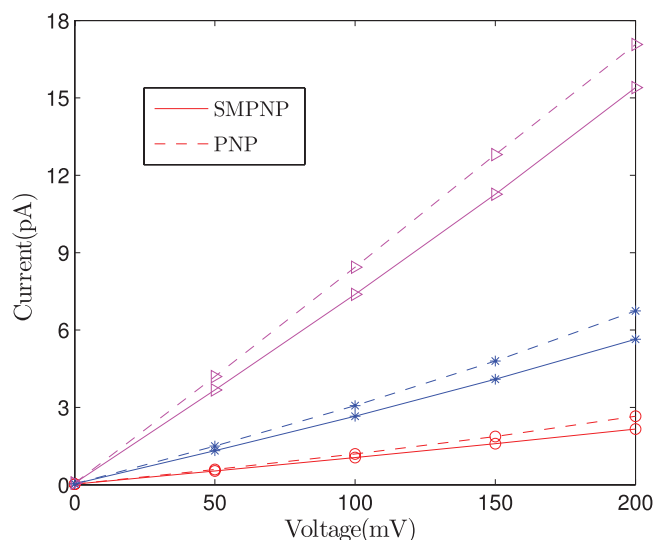


FIG. 5. Ion current through a gramicidin A channel without size effect and with size effects $a_0 = 3.1 \text{ \AA}$, $a_1 = 2.3 \text{ \AA}$, and $a_2 = 2.4 \text{ \AA}$ under three different bulk concentrations: 2.0M (triangle), 0.5M (star), and 0.1M (circle). The three solid lines show the results with ionic size effects while the dashed lines show results without ionic size effects.

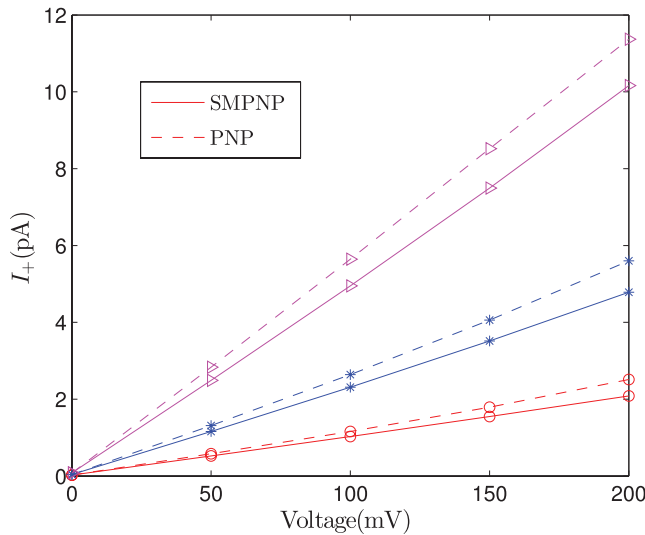
for SMPNP model and

$$I_z = - \sum_{i=1}^K q_i \int D_i \left(\frac{\partial c_i}{\partial z} + \frac{q_i}{k_B T} c_i \frac{\partial \phi}{\partial z} \right) dx dy \quad (55)$$

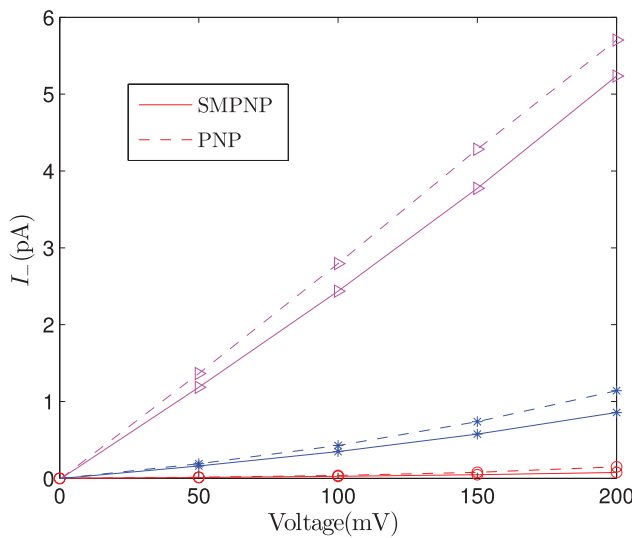
for PNP model, where c_i and ϕ are the unknowns we need to solve from SMPNP or PNP equations. The integration is taken over a given plane at z -position and perpendicular to the pore axis and shows slight differences for different z values.³⁸ Here, gA channel is simulated under a variety of membrane voltages (0 mV, 50 mV, 100 mV, 150 mV, and 200 mV) and bulk ionic concentrations (0.1M, 0.5M, and 2.0M) using SMPNP and PNP. The current across $z = 0$ plane is calculated.

Figure 5 illustrates the currents across the gA channel versus voltages in different bulk concentrations. For both models, the I - V curves show the same upward tendency as voltage increases. The current values obtained with SMPNP model are apparently smaller than those obtained from PNP model under same conditions. Around 10% decrease of current is observed from the figure for the given boundary conditions.

To further investigate ion current across channel, we plot the current of positive and negative ion (denoted by I_+ and I_-) in Figure 6. The attenuation of current can also be seen in both subfigures when size effects are incorporated. At low bulk ionic concentration (e.g., 0.1M), the negative ion flux is much smaller compared to the positive ion flux. This is because gA channel is selective for potassium (positive) ions. Besides, the percentage of negative ion flux in the whole current increases as bulk concentration increases, but the positive ion flux still plays a leading role.



(a)



(b)

FIG. 6. Current contribution of (a) positive ion and (b) negative ion in PNP and SMPNP models.

From the current formula defined by Eq. (54), we define diffusion component in SMPNP model

$$I_{diff} = - \sum_{i=1}^K q_i \int D_i \left(\frac{\partial c_i}{\partial z} + \frac{k_i c_i}{1 - \sum_l a_l^3 c_l} \sum_l a_l^3 \frac{\partial c_l}{\partial z} \right) dx dy \quad (56)$$

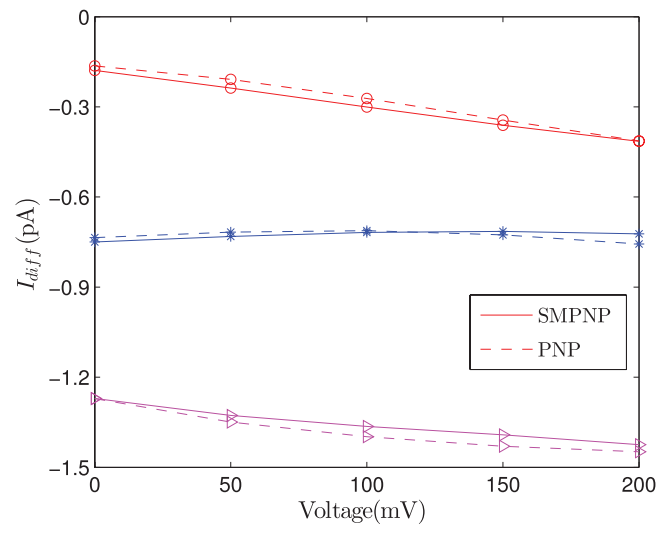
and the drift term

$$I_{drift} = - \sum_{i=1}^K q_i \int D_i \frac{q_i}{k_B T} c_i \frac{\partial \phi}{\partial z} dx dy. \quad (57)$$

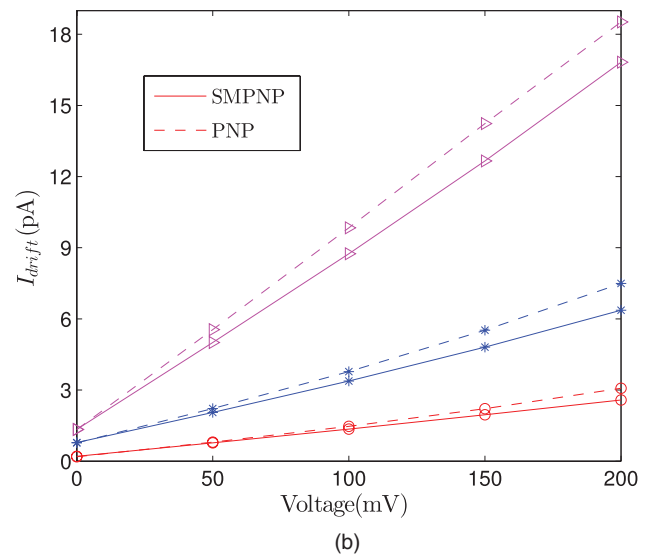
For PNP, the diffusion term is

$$I_{diff} = - \sum_{i=1}^K q_i \int D_i \frac{\partial c_i}{\partial z} dx dy, \quad (58)$$

and the drift term is defined as the same as in Eq. (57). The ion currents calculated from diffusion term and drift term are plotted in Figure 7. Figure 7(a) shows that the diffusion term has a negative contribution to the total currents, and ionic



(a)



(b)

FIG. 7. Current contribution of (a) diffusion term and (b) drift term in PNP and SMPNP models.

size effects impose little influence on current from diffusion. In addition, with increase of the applied voltage, the current from diffusion term does not change much. Whereas the contribution of drift term to current illustrated in Figure 7(b) is observed to have a leading role in the whole current. This subfigure has nearly the same shapes of the total I - V curves.

At last, the additional diffusion components of Eq. (54) for SMPNP model can be extracted and denoted as

$$I_{size} = - \sum_{i=1}^K q_i \int D_i \frac{k_i c_i}{1 - \sum_l a_l^3 c_l} \sum_l a_l^3 \frac{\partial c_l}{\partial z} dx dy. \quad (59)$$

The current I_{size} are plotted in Figure 8. With increase of the applied voltage, the absolute value of I_{size} gradually increases, but keeps tiny negative values ($\sim -10^{-3}$ pA in current simulations) compared to the total current. From above observations, it is indicated that the ionic size effects to the total current in a channel from SMPNP model are mainly conveyed through the drift term.

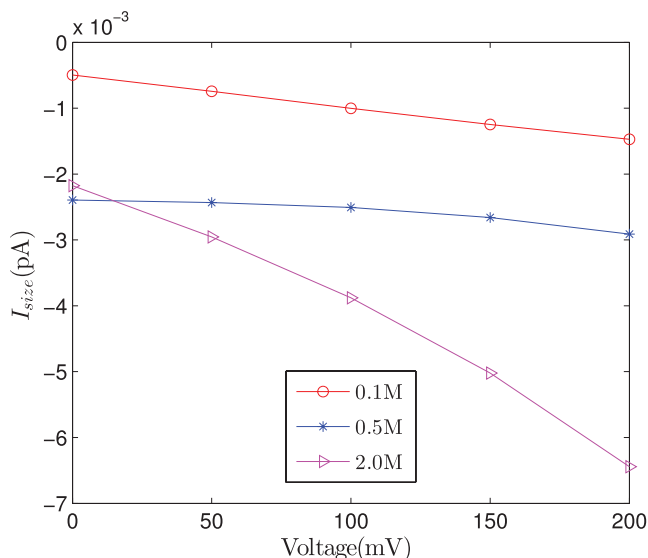


FIG. 8. Current contribution of the additional diffusion terms appeared in SMPNP (the second term in Eq. (54)).

IV. CONCLUSION

We have investigated the ionic size effects to biomolecular solvation energy and ion current across a channel by using the nonuniform SMPNP. We paid special attentions on the nonuniform size model and numerical calculations on real protein systems, which is rarely explored in literatures for a class of recently studied size-modified PB and PNP models.

The electrostatic free energy is studied in the first place, as well as the widely used approximation form in PB community. By using Taylor expansions of the concentrations with respect to potential, a convenient approximate formulation is found for the general nonuniform size-modified PNP/PB solvation energy calculation. The formulation is similar as in usual PB energy calculations, but with a lower order approximation. Numerical calculations on spherical cavity, DNA, and AChE systems demonstrate that the approximate energy calculations result in small differences from the accurate ones, indicating that the approximate form is also effective as well for the SMPNP/SMPB models. Besides, the salt dependence of solvation energy with size effects is given for the 1:1 symmetric solution, and when all ionic sizes are identical, it can be reduced to the known relation. Though a decay of solvation energy with increasing of the ionic strength cannot be proved rigorously for the general nonuniform size model, all of our numerical calculations seem to support the phenomenon. In addition, solvation energy calculated from SMPB is higher than the PB one, which can be physically explained by the reduced screening effect resulted from the ionic size effects.

In ion channel simulating, the size effects to ion current across a channel are investigated in detail. Numerical tests are implemented on gA channel in different bulk concentrations and voltages. It is observed that ion current calculated from SMPNP is smaller than that from PNP. Numerical experiments show that the drift term has a leading contribution to the total current in both PNP and SMPNP simulations, and the size effects to the current are also mainly conveyed through the drift term.

ACKNOWLEDGMENTS

The work was supported by the State Key Laboratory of Scientific/Engineering Computing, National Center for Mathematics and Interdisciplinary Sciences, the Chinese Academy of Sciences, and the China NSF (91230106).

- ¹B. Lu and Y. C. Zhou, *Biophys. J.* **100**, 2475 (2011).
- ²I. Borukhov, D. Andelman, and H. Orland, *Phys. Rev. Lett.* **79**, 435 (1997).
- ³N. A. Baker, "Biomolecular applications of Poisson–Boltzmann methods," *Reviews in Computational Chemistry* (John Wiley & Sons, Inc., 2005), pp. 349–379.
- ⁴F. Fogolari, A. Brigo, and H. Molinari, *J. Mol. Recognit.* **15**, 377 (2002).
- ⁵B. Lu, Y. Zhou, M. J. Holst, and J. A. McCammon, *Commun. Comput. Phys.* **3**, 973 (2008).
- ⁶M. K. Gilson, M. E. Davis, B. A. Luty, and J. A. McCammon, *J. Phys. Chem.* **97**, 3591 (1993).
- ⁷B. Eisenberg, *Biophys. J.* **104**, 1849 (2013).
- ⁸M. S. Kilic, M. Z. Bazant, and A. Ajdari, *Phys. Rev. E* **75**, 021502 (2007).
- ⁹M. S. Kilic, M. Z. Bazant, and A. Ajdari, *Phys. Rev. E* **75**, 021503 (2007).
- ¹⁰R. R. Netz and H. Orland, *Eur. Phys. J. E* **1**, 203 (2000).
- ¹¹J.-L. Liu and B. Eisenberg, *J. Phys. Chem. B* **117**, 12051 (2013).
- ¹²G. Tresset, *Phys. Rev. E* **78**, 061506 (2008).
- ¹³I. Borukhov, D. Andelman, and H. Orland, *Electrochim. Acta* **46**, 221 (2000).
- ¹⁴K. A. Sharp and B. Honig, *J. Phys. Chem.* **94**, 7684 (1990).
- ¹⁵A. R. J. Silalahi, A. H. Boschitsch, R. C. Harris, and M. O. Fenley, *J. Chem. Theory Comput.* **6**, 3631 (2010).
- ¹⁶V. B. Chu, Y. Bai, J. Lipfert, D. Herschlag, and S. Doniach, *Biophys. J.* **93**, 3202 (2007).
- ¹⁷A. H. Boschitsch and P. V. Danilov, *J. Comput. Chem.* **33**, 1152 (2012).
- ¹⁸K. A. Sharp, R. A. Friedman, V. Misra, J. Hecht, and B. Honig, *Biopolymers* **36**, 245 (1995).
- ¹⁹K. A. Sharp, *Biopolymers* **36**, 227 (1995).
- ²⁰R. C. Harris, J. H. Bredenberg, A. R. J. Silalahi, A. H. Boschitsch, and M. O. Fenley, *Biophys. Chem.* **156**, 79 (2011).
- ²¹R. C. Harris, A. H. Boschitsch, and M. O. Fenley, *J. Chem. Phys.* **140**, 075102 (2014).
- ²²B. Li, *SIAM J. Math. Anal.* **40**, 2536 (2009).
- ²³B. Li, *Nonlinearity* **22**, 811 (2009).
- ²⁴S. Zhou, Z. Wang, and B. Li, *Phys. Rev. E* **84**, 021901 (2011).
- ²⁵J. Wen, S. Zhou, Z. Xu, and B. Li, *Phys. Rev. E* **85**, 041406 (2012).
- ²⁶B. Li, P. Liu, Z. Xu, and S. Zhou, *Nonlinearity* **26**, 2899 (2013).
- ²⁷B. Wallace, *Biophys. J.* **49**, 295 (1986).
- ²⁸B. Wallace, *J. Struct. Biol.* **121**, 123 (1998).
- ²⁹D. A. Doyle, J. M. Cabral, R. A. Pfuetzner, A. Kuo, J. M. Gulbis, S. L. Cohen, B. T. Chait, and R. MacKinnon, *Science* **280**, 69 (1998).
- ³⁰L. Song, M. R. Hobauch, C. Shustak, S. Cheley, H. Bayley, and J. E. Gouaux, *Science* **274**, 1859 (1996).
- ³¹R. R. Ketchum, B. Roux, and T. A. Cross, *Structure* **5**, 1655 (1997).
- ³²B. Eisenberg, *Acc. Chem. Res.* **31**, 117 (1998).
- ³³D. Marx and J. Hutter, *Modern Methods and Algorithms of Quantum Chemistry* (John von Neumann Institute for Computing, Jülich, 2000), pp. 329–477.
- ³⁴H. Hwang, G. C. Schatz, and M. A. Ratner, *J. Phys. Chem. A* **111**, 12506 (2007).
- ³⁵S. C. Li, M. Hoyle, S. Kuyucak, and S.-H. Chung, *Biophys. J.* **74**, 37 (1998).
- ³⁶B. Corry, S. Kuyucak, and S.-H. Chung, *Biophys. J.* **78**, 2364 (2000).
- ³⁷M. G. Kurnikova, R. D. Coalson, P. Graf, and A. Nitzan, *Biophys. J.* **76**, 642 (1999).
- ³⁸B. Tu, M. Chen, Y. Xie, L. Zhang, B. Eisenberg, and B. Lu, *J. Comput. Chem.* **34**, 2065 (2013).
- ³⁹D. S. Bolintineanu, A. Sayyed-Ahmad, H. T. Davis, and Y. N. Kaznessis, *PLoS Comput. Biol.* **5**, e1000277 (2009).
- ⁴⁰D. Chen, J. Lear, and B. Eisenberg, *Biophys. J.* **72**, 97 (1997).
- ⁴¹U. M. B. Marconi and P. Tarazona, *J. Chem. Phys.* **110**, 8032 (1999).
- ⁴²T.-L. Horng, T.-C. Lin, C. Liu, and B. Eisenberg, *J. Phys. Chem. B* **116**, 11422 (2012).
- ⁴³B. Eisenberg, T.-L. Horng, T.-C. Lin, and C. Liu, *Biophys. J.* **104**, 509a (2013).
- ⁴⁴B. Eisenberg, Y. Hyon, and C. Liu, *J. Chem. Phys.* **133**, 104104 (2010).
- ⁴⁵I. Klapper, R. Hagstrom, R. Fine, K. Sharp, and B. Honig, *Protein* **1**, 47 (1986).

- ⁴⁶W. Im, D. Beglov, and B. Roux, *Comput. Phys. Commun.* **111**, 59 (1998).
- ⁴⁷N. A. Baker, D. Sept, S. Joseph, M. J. Holst, and J. A. McCammon, *Proc. Natl. Acad. Sci. U.S.A.* **98**, 10037 (2001).
- ⁴⁸L. B. Zhang, *Numer. Math. Theor. Methods Appl.* **2**, 65 (2009).
- ⁴⁹M. Chen and B. Lu, *J. Chem. Theory Comput.* **7**, 203 (2011).
- ⁵⁰M. Chen, B. Tu, and B. Lu, *J. Mol. Graph. Model.* **38**, 411 (2012).
- ⁵¹H. Si, Tetgen: a quality tetrahedral mesh generator and a 3D Delaunay triangulator, see <http://www.tetgen.org>.
- ⁵²I.-L. Chern, J.-G. Liu, and W.-C. Wang, *Methods Appl. Anal.* **10**, 309 (2003).
- ⁵³B. Lu, M. J. Holst, J. A. McCammon, and Y. C. Zhou, *J. Comput. Phys.* **229**, 6979 (2010).
- ⁵⁴Y. Xie, J. Cheng, B. Lu, and L. Zhang, *Mol. Based Math. Biol.* **1**, 90 (2013).